



ELSEVIER

Computer Physics Communications 147 (2002) 427–430

Computer Physics  
Communications

www.elsevier.com/locate/cpc

# Crossover effects in the bond-diluted Ising model in three dimensions

P.E. Berche<sup>a,\*</sup>, C. Chatelain<sup>b</sup>, B. Berche<sup>c</sup>, W. Janke<sup>b</sup>

<sup>a</sup> *Groupe de Physique des Matériaux, Université de Rouen, F-76821 Mont Saint-Aignan Cedex, France*

<sup>b</sup> *Institut für Theoretische Physik, Universität Leipzig, Augustusplatz 10/11, D-04109 Leipzig, Germany*

<sup>c</sup> *Laboratoire de Physique des Matériaux, Université Henri Poincaré, BP 239, F-54506 Vandoeuvre-les-Nancy Cedex, France*

## Abstract

We investigate by Monte Carlo simulations the critical properties of the three-dimensional bond-diluted Ising model. The phase diagram is determined by locating the maxima of the magnetic susceptibility and is compared to mean-field and effective-medium approximations. The calculation of the size-dependent effective critical exponents shows the competition between the different fixed points of the model as a function of the bond dilution. © 2002 Elsevier Science B.V. All rights reserved.

PACS: 64.60.Cn; 05.50.+q; 05.70.Jk; 64.60.Fr

Keywords: Critical phenomena; Ising model; Disorder; Monte Carlo simulations

## 1. Introduction

The qualitative influence of quenched disorder at second-order phase transitions is well understood since Harris proposed a relevance criterion [1] based on the knowledge of the specific heat critical exponent  $\alpha_{\text{pure}}$  of the pure model: when  $\alpha_{\text{pure}}$  is positive, the disordered system will reach a new fixed point with new critical exponents whereas if  $\alpha_{\text{pure}}$  is negative, the same universality class will persist.

As a paradigmatic model, the three-dimensional (3D) disordered Ising model characterized by  $\alpha_{\text{pure}} = 0.109(4)$  has been extensively studied by:

- Renormalization group methods in the weak quenched dilution regime. The best estimates for the critical exponents obtained by this method are [2]:

$$\nu = 0.678 \pm 0.010,$$

$$\eta = 0.030 \pm 0.003,$$

$$\gamma = 1.330 \pm 0.017.$$

- Monte Carlo simulations of the site-diluted case for which the following exponents have been found [3]:

$$\nu = 0.6837 \pm 0.0053,$$

$$\beta = 0.3546 \pm 0.0028,$$

$$\gamma = 1.342 \pm 0.010.$$

- Experimental investigations.  
For a review of these different results, see Ref. [4].

\* Corresponding author.

E-mail address: pierre.berche@univ-rouen.fr (P.E. Berche).

The general picture which is now widely accepted is that, starting from the pure Ising model (with exponents  $\nu = 0.6304 \pm 0.0013$ ,  $\gamma = 1.2396 \pm 0.0013$ ,  $\beta = 0.3258 \pm 0.0014$ , see Ref. [5]), the critical temperature decreases and eventually vanishes at the percolation threshold below which there is no longer any long-range order in the system, due to the absence of percolating clusters. In the dilution-temperature plane, the critical line  $T_c(p)$  which delimits ferromagnetic and paramagnetic phases has two end-points (namely the pure system and the percolation point) described by unstable fixed points and it is commonly believed that the quenched disordered system has universal properties described by a unique stable fixed point. According to this picture, the competition between fixed points possibly leads to an effective variation of universal critical quantities.

In this paper, we first determine the phase diagram of the bond-diluted problem (up to now, only the site-diluted case has been studied) and compare it to a prediction in the single-bond effective-medium approximation and then we try to illustrate the competition between fixed points leading to crossover regimes in some physical quantities.

## 2. Phase diagram

The bond-diluted Ising model is defined by the following Hamiltonian with independent quenched random interactions:

$$-\beta H = \sum_{(i,j)} K_{ij} \delta_{\sigma_i, \sigma_j} \quad (\sigma_i = \pm 1). \quad (1)$$

The coupling strengths are allowed to take two different values  $K_{ij} = K \equiv J/k_B T$  and 0 with probabilities  $p$  and  $1 - p$ , respectively,

$$P(K_{ij}) = p\delta(K_{ij} - K) + (1 - p)\delta(K_{ij}), \quad (2)$$

$c = 1 - p$  being the concentration of missing bonds, which play the role of the non-magnetic impurities. The simulation technique is based on the Swendsen–Wang cluster algorithm with periodic boundary conditions in the three space directions.

The phase diagram is obtained numerically from the maxima of a diverging quantity (Fig. 1). Here we choose the susceptibility, since the stability of the disordered fixed point implies that the specific-heat exponent is negative in the random system.

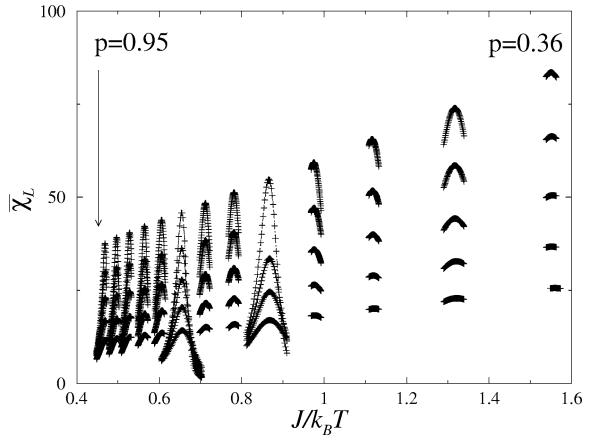


Fig. 1. Variation of the average magnetic susceptibility  $\bar{\chi}_L$  versus the coupling strength  $K = J/k_B T$  for several concentrations  $p$  and  $L = 8, 10, 12, 14, 16, 18, 20$ . For each value of  $p$  and each size, only one value of  $K$  has been simulated: the extension of the  $K$  values has been obtained by the standard histogram reweighting technique.

Thus, the error in this quantity is larger than for the susceptibility. The percolation threshold is located at  $p_c \approx 0.2488$ .

To get an accurate determination of the maxima of the susceptibility, we used the histogram reweighting technique with 2500 Monte Carlo sweeps (MCS) and between 2500 and 5000 samples of disorder. The number of Monte Carlo sweeps is justified by the increasing behaviour of the energy autocorrelation time and we chose for each size at least 250 independent measurements of the physical quantities ( $N_{MCS} > 250\tau_E$ ).

For a second-order phase transition, the autocorrelation time is expected to behave as  $L^z$  at the critical point where  $z$  is the dynamical critical exponent (Fig. 2). For the disordered Ising model, we get the values of  $z$  shown in Table 1. We see that the critical slowing down weakens for the disordered model and becomes smaller when the concentration of magnetic bonds  $p$  decreases, but it is necessary to increase the number of disorder realizations when  $p$  decreases because of the vicinity of the percolation threshold.

In order to check the quality of the averaging techniques, we can study the stability of the susceptibility for the largest size considered versus the number of Monte Carlo sweeps involved in the thermal average. The results are given in Table 2 for different samples as well as for the disorder average. With 2500 MCS, the accuracy of the results for a given sample is not

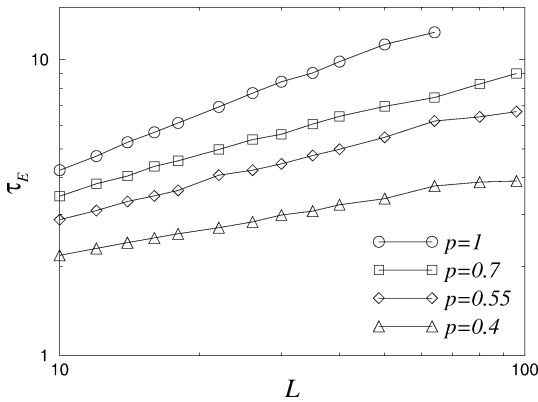


Fig. 2. Variation on a log-log scale of the energy autocorrelation time  $\tau_E$  versus the size  $L$  of the system. The energy autocorrelation time increases with the concentration of magnetic bonds  $p$  and its greatest value obtained for  $L = 96$ ,  $p = 0.7$  is around 9.

Table 1  
The dynamical critical exponent  $z$  as obtained from linear fits of  $\log \tau_E$  vs  $\log L$

$p$	1	0.7	0.55	0.4
$z$	0.59	0.41	0.38	0.27

Table 2  
Evolution of the susceptibility with the number of Monte Carlo sweeps per spin for different samples,  $\chi_j$ , and the average value (with 2500 samples) at  $L = 96$ ,  $p = 0.7$

# MCS	$\chi_1$	$\chi_2$	$\chi_3$	$\chi_4$	$\chi_5$	$\bar{\chi}$
100	1268	720	1141	939	833	1058
500	1272	1520	1223	1029	953	1210
1000	1262	1544	1205	1068	911	1219
1500	1282	1433	1277	1047	915	1227
2000	1332	1441	1221	1073	917	1235
2500	1358	1484	1234	1012	1014	1234

perfect, of course, but the precision of the average over disorder is quite good on the other hand. The disorder average procedure has been investigated by computing the susceptibility  $\chi_j$  for different samples,  $1 \leq j \leq N_s$ , where  $N_s$  is the total number of samples (Fig. 3). We can see that the dispersion of the values of  $\chi$  is not very large because the fluctuations in the average value disappear after a few hundreds realizations.

The phase diagram obtained from the location of the maxima of the susceptibility for the largest lattice size as a function of the concentration of magnetic bonds is shown in Fig. 4. The simple mean-

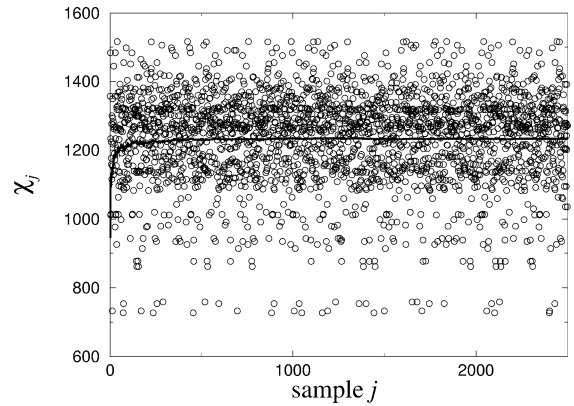


Fig. 3. Distribution of the susceptibility for the different disorder realizations of the Ising model with  $L = 96$  and a concentration of magnetic bonds  $p = 0.7$ . The average value over the samples  $\bar{\chi}$  is shown by the black line.

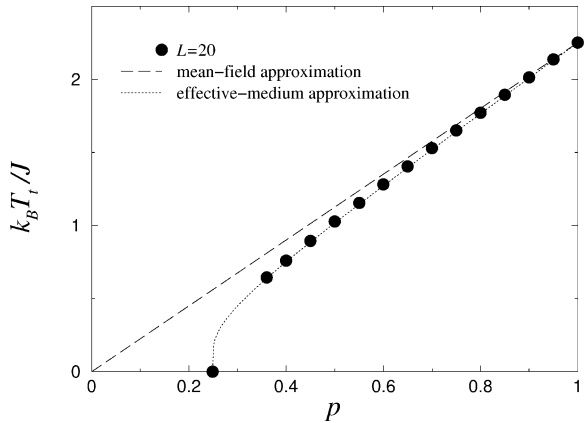


Fig. 4. Phase diagram of the 3D bond-diluted Ising model compared with the mean-field and effective-medium approximations.

field transition temperature is drawn for comparison: it gives a linear behaviour as a function of the bond concentration  $p$  and we can check that this approximation holds only in the low-dilution regime,  $p > 0.8$ . On the other hand, the effective-medium approximation [6] gives very good agreement with the simulated transition line. Treating only a single bond in an effective medium leads to the following relation for the critical coupling:

$$K_c(p) = \ln \frac{(1 - p_c)e^{K_c(1)} - (1 - p)}{p - p_c} \quad (3)$$

This relation is exact in the vicinity of both the pure system and the percolation threshold.

### 3. Competition between the fixed points

The main problem encountered in previous studies of the disordered Ising model was the question of measuring effective or asymptotic exponents. Although the change of universality class should happen theoretically for an arbitrarily low disorder, it can be very difficult to measure the new critical exponents because the asymptotic behaviour cannot always be reached practically. Another difficulty comes from the vicinity of the ratios  $\gamma/\nu$  and  $\beta/\nu$  in the pure and disordered universality classes. Indeed, these values for the pure model are [5]:

$$\gamma/\nu = 1.966(6), \quad \beta/\nu = 0.517(3), \\ \nu = 0.6304(13),$$

and for the disordered Ising model [3]:

$$\gamma/\nu = 1.96(3), \quad \beta/\nu = 0.519(8), \quad \nu = 0.6837(53).$$

Thus, from standard finite-size scaling techniques, the critical exponent  $\nu$  only will allow us to discriminate between the two fixed points. This exponent can be evaluated from the finite-size scaling of the derivative of the magnetization versus the temperature which is expected to behave as  $d \ln m / dK \sim L^{1/\nu}$ . From this power-law behaviour, we have extracted the effective size-dependent exponent  $(1/\nu)_{\text{eff}}$  which is plotted against  $1/L_{\text{min}}$  for different bond concentrations  $p$  in

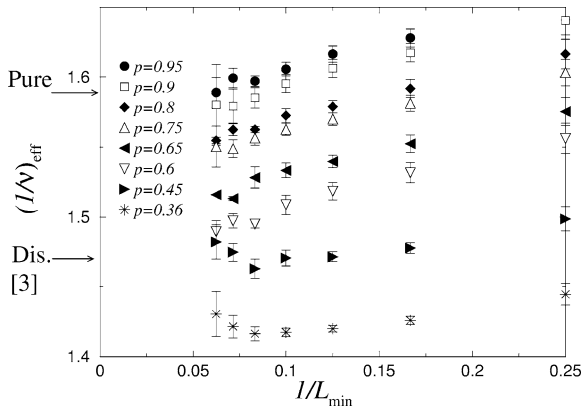


Fig. 5. Effective exponents  $(1/\nu)_{\text{eff}}$  as a function of  $1/L_{\text{min}}$  for  $p = 0.95, 0.9, 0.8, 0.75, 0.65, 0.6, 0.45$  and  $0.36$ . The error bars correspond to the standard deviations of the power-law fits. The arrows indicate the values of  $1/\nu$  for the pure model [5] and the site-diluted one [3].

Fig. 5 where  $L_{\text{min}}$  is the smallest lattice size used in the fits.

We clearly see that in the regime of low dilution ( $p$  close to 1), the system is influenced by the pure fixed point. On the other hand, when the bond concentration is small, the vicinity of the percolation fixed point induces a decrease of  $1/\nu$  below its expected disordered value. Indeed, the percolation fixed point is characterized by  $1/\nu \sim 1.12$  [7].

### 4. Conclusion

We have presented, from a numerical study, the influence of bond dilution on the critical properties of the 3D Ising model. The universality class of the disordered model is modified by disorder but its precise characterization is difficult because of the competition between the different fixed points which induce crossover effects, even for relatively large lattice sizes. The next step is to accurately locate the best dilution which minimizes these crossover effects.

### Acknowledgements

We gratefully acknowledge financial support by the DAAD and EGIDE through the PROCOPE exchange programme. C.C. thanks the EU network “Discrete Random Geometries: from solid state physics to quantum gravity” for a postdoctoral grant. This work was supported by the computer-time grants 2000007 of the Centre de Ressources Informatiques de Haute-Normandie (CRIHAN) and hlz061 of NIC, Jülich.

### References

- [1] A.B. Harris, J. Phys. C 7 (1974) 1671.
- [2] A. Pelissetto, E. Vicari, Phys. Rev. B 62 (2000) 6393.
- [3] H.G. Ballesteros, L.A. Fernández, V. Martín-Mayor, A. Muñoz Sudupe, G. Parisi, J.J. Ruiz-Lorenzo, Phys. Rev. B 58 (1998) 2740.
- [4] R. Folk, Y. Holovatch, T. Yavors’kii, cond-mat/0106468.
- [5] R. Guida, J. Zinn-Justin, J. Phys. A 31 (1998) 8103.
- [6] L. Turban, Phys. Lett. 75A (1980) 307.
- [7] C.D. Lorenz, R.M. Ziff, Phys. Rev. E 57 (1998) 230.